Talanta 104 (2013) 116–121

Contents lists available at SciVerse ScienceDirect

Talanta

journal homepage: www.elsevier.com/locate/talanta

A novel mesoporous silica nanosphere matrix for the immobilization of proteins and their applications as electrochemical biosensor

Juan Li, Xingzhang Qin, Zhanjun Yang, Huamei Qi, Qin Xu, Guowang Diao *

College of Chemistry and Chemical Engineering, Yangzhou University; Jiangsu Key Laboratory of Environmental Engineering and Monitoring, Yangzhou 225002, PR China

ARTICLE INFO

Article history:
Received 27 July 2012
Received in revised form
14 November 2012
Accepted 17 November 2012
Available online 24 November 2012

Keywords:
Mesoporous silica nanosphere
Direct electrochemistry
Glucose oxidase
Glucose
Biosensor

ABSTRACT

A mesoporous silica nanoshpere (MSN) was proposed to modify glassy carbon electrode (GCE) for the immobilization of protein. Using glucose oxidase (GOD) as a model, direct electrochemistry of protein and biosensing at the MSN modified GCE was studied for the first time. The MNS had large surface area and offered a favorable microenvironment for facilitating the direct electron transfer between enzyme and electrode surface. Scanning electron microscopy, transmission electron microscopy, UV–vis spectroscopy and cyclic voltammetry were used to examine the interaction between GOD and the MSN matrix. The results demonstrated that the immobilized enzyme on the MSN retained its native structure and bioactivity. In addition, the electrochemical reaction showed a surface controlled, reversible two-proton and two-electron transfer process with the apparent electron transfer rate constant of 3.96 s^{-1}. The MNS-based glucose biosensor exhibited the two linear ranges of 0.04–2.0 mM and 2.0–4.8 mM, a high sensitivity of 14.5 mA M^{-1} cm^{-2} and a low detection limit of 0.02 mM at signal-to-noise of 3. The proposed biosensor showed excellent selectivity, good reproducibility, acceptable stability and could be successfully applied in the reagentless detection of glucose in real samples at −0.45 V. The work displayed that mesoporous silica nanosphere provided a promising approach for immobilizing proteins and fabrication of excellent biosensors.

1. Introduction

Since the discovery of MCM-41-type ordered mesoporous silica by Mobil corporation scientists in 1992, a large amount of research has been conducted on its controlled syntheses and applications [1]. Due to good biocompatibility [2,3], stable mesoporous structures, large surface areas, and tunable pore sizes and volumes, MCM-type mesoporous silica materials have made them ideal candidate for hosting molecules of various sizes, shapes and functionalities [4]. In particular, mesoporous silica nanoparticles have attracted great attention in many research fields over the past few years [5]. Great endeavors have been made for the use of mesoporous silica nanoparticles in controlled drug/gene release and as delivery carriers [6–11], biosensors [12,13], biomarkers [14,15] and enzyme supporters [3,16,17]. As a protein immobilizing matrix, mesoporous materials can incorporate proteins through physical or chemical action with good adsorption due to its large specific surface area [16]. The incorporation of mesoporous materials into redox enzymes could provide an active biomaterial [18]. Lin's group for the first time synthesized a novel mesoporous silica nanosphere (MSN), which was further used to construct a controlled-release delivery system for pharmaceutical drug molecules and neurotransmitters [4]. To the best of our knowledge, MSN has been not used for immobilization of proteins for applications in electrochemical biosensing.

The detection of blood glucose levels is of great importance for the diagnosis and therapy of diabetics. Glucose oxidase (GOD) as an ideal mode enzyme has been extensively used in fabrication of electrochemical glucose biosensors due to its catalytic ability to oxidize glucose [19–22]. However, an ultimate goal of glucose sensing is to develop the third generation biosensor based on the direct electron transfer (DET) between the cofactor FAD of GOD and the electrode surface without the mediator [23]. Unfortunately, the redox center in biomolecules is usually seated deeply in cavity of the enzyme molecules, which makes it hard to realize DET of enzyme to the electrode [24]. Thus, many novel nanomaterials, such as gold nanoparticles [25,26] carbon nanotubes [27–30], graphene [31,32], titanium oxide [33] and tin disulfide [34] have been explored to immobilize GOD for accelerating DET of redox enzyme on the surface of electrode.

In this work, MSN was synthesized according to previous method with some modifications. By immobilizing GOD on MNS modified electrode, a novel electrochemical biosensor was constructed. The MNS materials have an average particle size of 115 nm and an average pore diameter of 2.3 nm. The large surface area, uniform porous structure and favorable microenvironment

* Corresponding author. Tel.: +86 514 87975587; fax: +86 514 87975244.
E-mail address: gwdiao@yzu.edu.cn (G. Diao).

0039-9140/$ - see front matter © 2012 Elsevier B.V. All rights reserved.
http://dx.doi.org/10.1016/j.talanta.2012.11.038

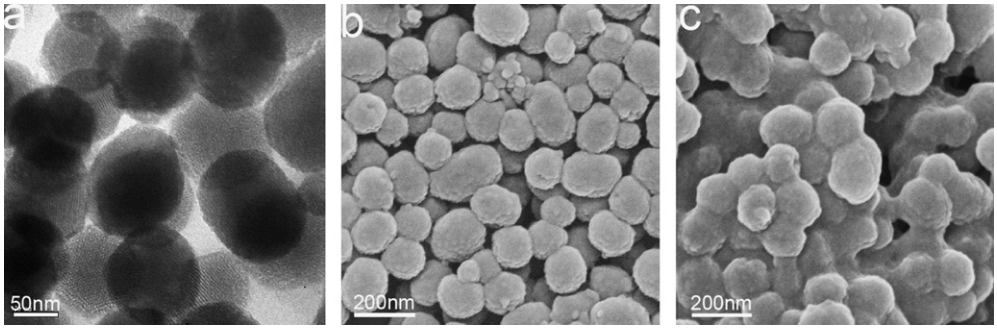

Fig. 1. (a) TEM image of MSN, (b) SEM images of MSN and (c) GOD–MSN.

facilitate the direct electron transfer between enzyme and electrode. A pair of obvious and well-defined redox peaks of GOD could be observed at the GOD–MSN/Nafion modified electrode. The resulting glucose biosensor showed high sensitivity, low detection limit, excellent selectivity and good reproducibility. Thus the mesoporous silica nanosphere provided a promising platform for immobilizing proteins for electrochemical biosensing.

2. Experimental

2.1. Reagents and materials

GOD (EC 1.1.3.4, 108 U mg^{-1}, from *Aspergillus niger*) was purchased from Amresco. D-(+)-Glucose and Nafion were purchased from Sigma-Aldrich. n-Cetyl-trimethylammonium bromide (CTAB) and tetramethoxysilane (TMOS) were supplied by Sinopharm Chemical Reagent Co., Ltd. A stock solution of D-glucose was prepared and allowed to mutarotate at room temperature for 24 h before use. Phosphate buffer solution (PBS) was 0.1 M Na_2HPO_4 and NaH_2PO_4 and its pH was adjusted with H_3PO_4 or NaOH solutions. All other chemicals and reagents are of analytical grade and were prepared using distilled water.

2.2. Apparatus

Electrochemical measurements were carried out on a CHI 852C electrochemical workstation (Co., CHI, USA). All experiments were performed with a three-electrode system using a glassy carbon electrode (GCE, Φ=3 mm) as the working electrode, a platinum wire as the auxiliary electrode and a saturated calomel electrode (SCE) as reference electrode. The cyclic voltammetry experiments were carried out at a scan rate of 100 mV s^{-1} in an electrochemical cell filled with 5.0 mL PBS. All pH measurements were made with S-25 digital pH-meter with glass combination electrode.

Transmission electron microscopy (TEM) images were obtained with a Philips Tecnai-12 transmission electron microscope (Holland) at an acceleration voltage of 100 kV. Scanning electron microscopy (SEM) images were obtained with a Hitachi S-4800 scanning electron microscope (Japan) at an acceleration voltage of 15 kV. UV–vis spectra were recorded using UV-2550 spectrophotometer (Shimadzu Co., Japan).

2.3. Synthesis of MCM-41-type mesoporous silica nanosphere

MCM-41-type mesoporous silica nanosphere was synthesized according to previous method with some modifications [4]. 0.2 g of CTAB was firstly dissolved in 96 mL of distilled water. 0.7 mL of NaOH (aqueous, 2.0 M) was added to CTAB solution, and then the solution temperature was adjusted to 80 °C. 1.0 mL of TMOS was added dropwise to the solution, and the mixture was allowed to stir for 2 h at 80 °C. Subsequently, the resulting white precipitate was isolated by filtration. After the silica particles were calcined at 550 °C for 5 h to remove the template, the mesoporous silica nanosphere was finally obtained.

2.4. Preparation of the GOD–MSN/Nafion/GCE

The GCE was firstly polished successively with 0.03 and 0.05 μm alumina slurry (Buhler) followed by rinsing thoroughly with distilled water, and finally sonicated in 1:1 nitric acid, acetone and distilled water and dried in air. 3.0 mg of MSN was dispersed in 1.0 mL of distilled water under ultrasonic stirring, and then 0.5 mL of the MSN suspension was mixed with equivalent volume of 8.0 mg mL^{-1} of GOD to form GOD–MSN mixed solution. Subsequently, 6.0 μL of the mixed solution was dropped on the surface of the pretreated GCE and dried in a desiccator. Finally, 5.0 μL of 0.5% Nafion solution was dropped on the surface of GOD–MSN/GCE to form GOD–MSN/Nafion modified electrode. The modified electrode was rinsed throughout with distilled water to wash away the loosely adsorbed enzyme molecules. The modified electrode was then stored in pH 7.0 PBS at 4 °C in a refrigerator before use.

3. Results and discussion

3.1. Characterizations of MSN, GOD and GOD–MSN

The TEM and SEM images of the synthesized mesoporous silica nanosphere shown in Fig. 1(a and b), indicate that MSN materials are composed of well-dispersed spherical nanoparticles with average diameter of 115 nm. The pore characterization of MSN was investigated by the N_2 isothermal adsorption experiments. The specific surface area, pore volume and average pore diameter were calculated to be 645.3 $m^2 g^{-1}$, 0.43 $cm^3 g^{-1}$ and 2.7 nm using the BET and BJH method, respectively. As can be seen from the TEM image, ordered mesopores and parallel channels appear. The uniform porous structure is advantageous to obtain a high enzyme loading. When GOD was immobilized in the MSN matrix, SEM image of the formed GOD–MSN (Fig. 1c) displayed uniform and homogeneous morphology.

The UV–vis absorption spectra of the MSN, native GOD and GOD–MSN were shown in Fig. 2. For the single MNS, no obvious peak was observed in the wavelength range of 200–700 nm, while the spectrum of GOD showed three characteristic absorption peaks. The absorption peak at 276 nm was ascribed to the characteristic of polypeptide chains, and the two weak peaks at 381 and 458 nm were attributed to the oxidized form of flavin group in protein structure [35]. The position and shape of absorption peaks of the GOD–MSN are almost the same as those

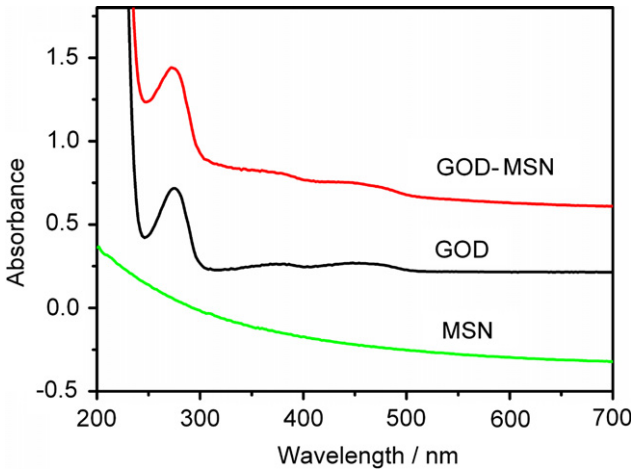

Fig. 2. UV–vis spectra of MSN, GOD and GOD–MSN.

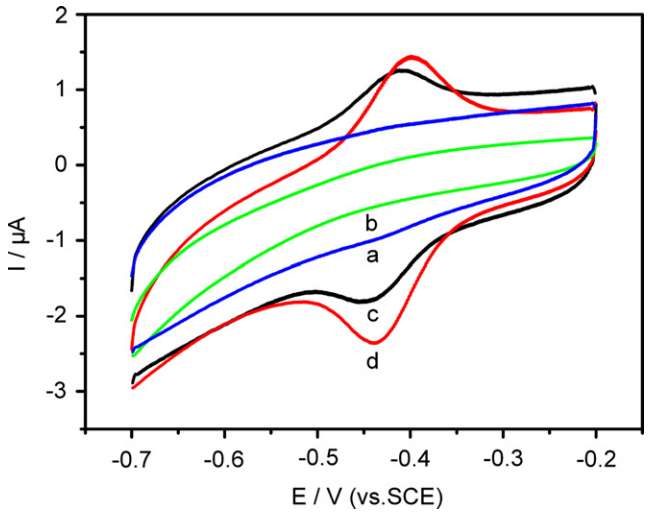

Fig. 3. (a) Cyclic voltammograms for Nafion/GCE, (b) MSN/Nafion/GCE, (c) GOD/Nafion/GCE, and (d) GOD–MSN/Nafion/GCE in N_2-saturated 0.1 M pH 6.5 PBS at a scan rate of 100 mV s^{-1}.

of the native GOD, indicating that the GOD immobilized in mesoporous silica nanosphere matrix indeed maintains its native structure.

3.2. The choice of experimental conditions for the glucose biosensor

Fig. S1 shows the cyclic voltammograms of the GOD–MSN/Nafion/GCE in N_2-saturated different concentrations of PBS solution. With the increasing of the concentration of PBS solution from 0.02 to 0.2 M, the reduction current increased to the maximum at 0.1 M and then decreased. The higher concentration of PBS solution produces high ion strength, which might result in the protein denaturation. Thus 0.1 M PBS was selected as the supporting electrolyte for glucose detection. The amount of GOD is another important factor affecting the analytical performance of the glucose biosensor. Fig. S2 illustrates the effect of different concentrations of GOD on the sensor response. With increase in GOD concentration the reduction current enhanced and reached the maximum at 8.0 mg mL^{-1} concentration. After the maximum concentration point the reduction current began to decrease. The higher loading of GOD might affect the mesoporous structure of MSN, thus hindering the direct electron transfer between the redox center of proteins and electrode surface.

3.3. Direct electrochemistry of GOD–MSN/Nafion modified GCE

The cyclic voltammograms of different modified GCEs in N_2-saturated PBS were shown in Fig. 3. No peaks were observed for the Nafion/GCE (curve a) and MSN/Nafion/GCE (curve b), while GOD/Nafion modified GCE (curve c) showed a pair of well-defined redox peaks. Compared with the GOD/Nafion/GCE, GOD immobilized on MSN matrix shows a pair of more distinct and well-defined redox peaks at −0.403 V and −0.438 V (curve d). Obviously, the MNS matrix can provide a favorable microenvironment to ensure more effective electrical contact between redox-active centers of enzyme and electrode surface, leading to the enhanced direct electrochemistry of GOD. The separation of peak potentials is 35 mV, which was smaller than 80 mV for GOD/graphene–chitosan/GCE [32] and 94 mV for GOD/Au/carbon paste electrode [36], indicating a faster electron transfer rate.

The effect of the scan rate on the cyclic voltammetric response at the GOD–MSN/Nafion modified GCE was shown in Fig. 4. The oxidation peak current (I_{pa}) and reduction peak current (I_{pc}) of the GOD–MSN/Nafion/GCE increased linearly with the increasing scan rate from 30 to 300 mV s^{-1} (inset I of Fig. 4), and the I_{pa}/I_{pc} ratio was approximately equal to 1, indicating that the redox reaction

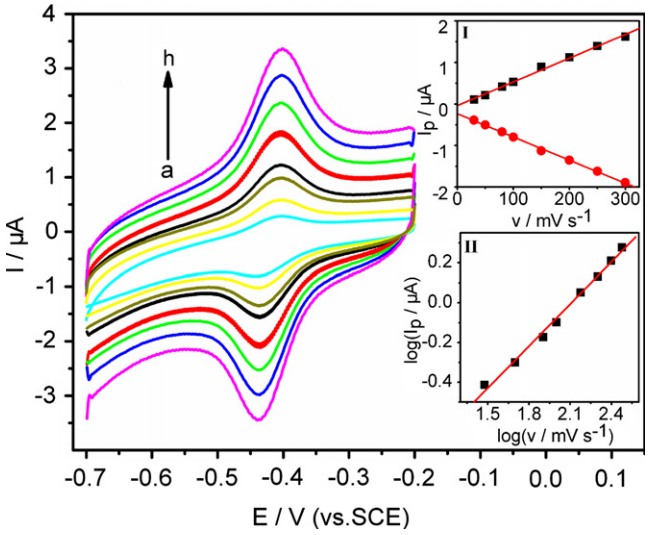

Fig. 4. Cyclic voltammograms of the GOD–MSN/Nafion/GCE in N_2-saturated 0.1 M pH 6.5 PBS at 30, 50, 80, 100, 150, 200, 250 and 300 mV s^{-1} (a–h). Inset I: plots of anodic and cathodic peak currents vs. scan rates; inset II: plot of logarithm of i_{pc} vs. logarithm of v^{-1}.

of GOD in MSN matrix is a surface-controlled process. The logarithm plot of cathodic peak current versus logarithm of the san rate shows a linear relationship (inset II of Fig. 4), which is very close to the theoretical slope for thin layer electrochemical behavior [37]. The surface coverage (Γ^*) of the electroactive GOD on surface of the modified electrode can be estimated according to the formula of $\Gamma^* = Q/nFA$. The surface coverage was calculated to be 2.07×10^{-11} mol cm^{-2}, which was larger than those of 1.60×10^{-11} mol cm^{-2} at GOD/SnS_2/Nafion/GCE [34], 9.8×10^{-12} mol cm^{-2} at GOD/Au nanoparticles/carbon paste electrode [36], 7.82×10^{-12} mol cm^{-2} at GOD/Au-dihexadecyl phosphate modified electrode [38] and 2.86×10^{-12} mol cm^{-2} at bare GCE [39]. According to Laviron's equation, the charge-transfer coefficient and the apparent electron transfer rate constant (k_s) for the proposed electrode were calculated to be 0.5 and 3.96 s^{-1}. The obtained value of k_s was larger than those of 2.42 s^{-1} at In_2O_3–chitosan [40], 1.56 s^{-1} at boron-doped carbon nanotubes [41], 1.7 s^{-1} at multi-walled carbon nanotubes [42] and 2.83 s^{-1} at graphene–chitosan modified GCEs [32]. This MSN matrix may

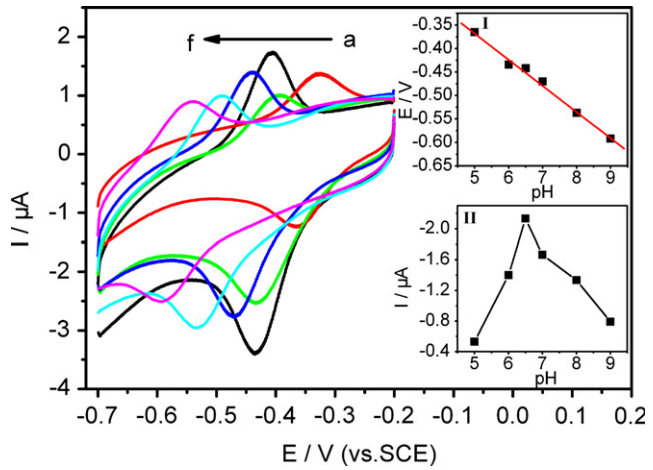

Fig. 5. Cyclic voltammograms of the GOD–MSN/Nafion/GCE in N_2-saturated PBS with different pH values of (a–f) 5.0, 6.0, 6.5, 7.0, 8.0 and 9.0 at a scan rate of 100 mV s^{-1}. Inset I: plot of formal potentials vs. pH; inset II: plot of peak currents vs. pH.

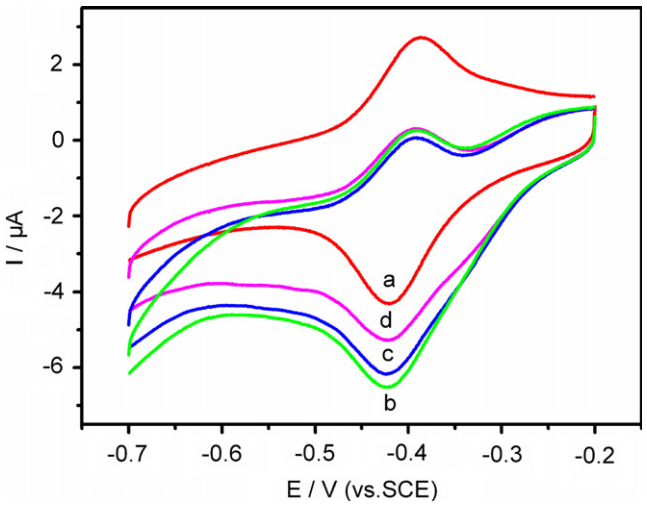

Fig. 6. Cyclic voltammograms of the GOD–MSN/Nafion/GCE in 0.1 M pH 6.5 N_2-saturated PBS (a), air-saturated PBS (b), air-saturated PBS including 0.5 mM (c) and 1.0 mM (d) glucose at a scan rate of 100 mV s^{-1}.

pierce the glycoprotein shell and more effectively shorten the distance between redox site of enzyme and the electrode surface, thus leading to the faster electron transfer.

The influence of the pH value on the electrochemical behavior of GOD on MSN matix was investigated and shown in Fig. 5. Both the cathodic and anodic peak potentials shifted negatively with the increase of pH from 4.0 to 8.0. Moreover, the redox potentials of GOD–MSN/Nafion/GCE changed linearly as a function of solution pH with a slope of -55.7 mV pH^{-1}, which was close to the theoretical value of -58.6 mV pH^{-1}. In addition the number of electron transferred in the electrochemical process was estimated to be 2 ($n \approx 1.7$, based on the formula of 59/n at 25 °C), thus indicating two protons and two electrons participating in the electron transfer process. Moreover, the peak currents reached its maximum value at pH 6.5 (inset II of Fig. 5), indicating an optimal pH for immobilized GOD.

3.4. Detection of glucose at the GOD–MSN/Nafion modified GCE

The cyclic voltammograms of the GOD–MSN/Nafion/GCE in oxygen-free PBS, air-saturated PBS and air-saturated PBS containing glucose were shown in Fig. 6. In air-saturated PBS, the cyclic voltammogram of the GOD–MSN/Nafion/GCE showed a great increase in reduction peak current and a simultaneous decrease in oxidation current (curve b). These results demonstrated that GOD ($FADH_2$) exerted an obvious electrocatalytic process toward the reduction of dissolved oxygen according to the Eqs. (1) and (2) [36].

$$GOD(FAD) + 2e^- + 2H^+ \leftrightarrow GOD(FADH_2) \quad (1)$$

$$GOD(FADH_2) + O_2 \rightarrow GOD(FAD) + H_2O_2 \quad (2)$$

$$Glucose + GOx(FAD) + O_2 \rightarrow Gluconolactone + GOx(FADH_2) \quad (3)$$

In the presence of oxygen, regenerated GOD (FAD) led to the increase of the reduction peak current of FAD. When the glucose was added into this system, it restrained the electrocatalytic reaction due to the enzyme-catalyzed reaction, thus reducing the concentration of GOD (FAD) as shown in the Eq. (3). So the reduction peak current of GOD decreased with the increase of glucose concentration (curves c and d). The glucose biosensor was therefore proposed based on the decease of the reduction peak current.

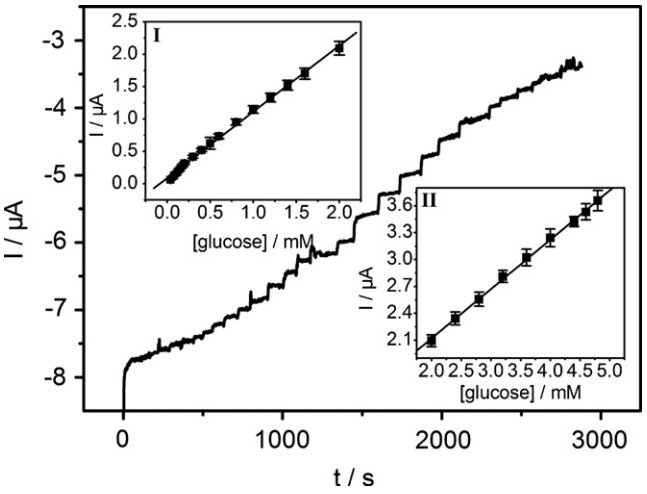

Fig. 7. Typical steady-state response of the GOD–MSN/Nafion/GCE on successive addition of glucose into air-saturated 0.1 M pH 6.5 PBS at -0.45 V applied potential, insets I and II: calibration curves of the GOD–MSN/Nafion/GCE for glucose.

Fig. 7 showed the typical amperometric response curves at GOD–MSN/Nafion modified GCE on successive injection of glucose to the air-saturated stirring PBS. The optimal potential and pH value for the amperomeric detection of glucose were chosen as -0.45 V and 6.5, respectively. The current response increased linearly with the increase of glucose concentration ranging from 0.04 to 2.0 mM with a correlation coefficient of 0.9971 and 0.2 to 4.8 mM with a correlation coefficient of 0.9986 (insets I and II of Fig. 7). The detection limit was 0.02 mM at signal-to-noise of 3. The sensitivity for the GOD–MSN/Nafion/GCE was calculated to be 14.5 mA M^{-1} cm^{-2}. The comparison of these analytical performances to those recent literatures of the glucose biosensor was shown in Table 1. These results demonstrated the highest sensitivity, extended linear range and reasonable detection limit were obtained with the GOD–MSN/Nafion/GCE. The apparent Michaelis–Menten constant (K_M^{app}) was calculated to be 4.7 mM for the glucose biosensor. The K_M^{app} value was smaller than those of 5.46, 11.6 and 37.6 mM reported by some literatures [49–51], indicating that the GOD immobilized in the MSN material has high affinity to glucose.

Table 1
Comparison of analytical performance between the GOD–MSN/Nafion/GCE and other enzyme electrodes.

Electrode	Applied potential (V)	Sensitivity ($mA\ M^{-1}\ cm^{-2}$)	Detection limit (mM)	Linear range (mM)	Reference
GOD–MSN/Nafion/GCE	−0.45	14.5	0.02	0.04–4.8	This work
MSCF[a]/GOD/Nafion–GCE	−0.40	–	0.035	0.05–5.0	[19]
GOD/SnS_2/Nafion/GCE	−0.45	7.6	0.01	0.025–1.1	[34]
GOD/CN*x*–MWNTs[b]	−0.50	13.0	0.01	0.02–1.02	[43]
GOD/In_2O_3–chitosan/GCE	−0.50	7.3	0.0019	0.05–1.3	[40]
GOD/gold nanorod/Pt electrode	+0.40	8.4	0.02	0.03–2.2	[44]
Nafion/GOD/Ag–Pdop[c]@CNT/GCE	−0.50	3.1	0.017	0.05–1.1	[45]
TiO_2/GOD/Nafion–GCE	−0.45	4.28	–	0.15–1.2	[33]
GOD/Pt/FCNA[d]/GCE	−0.08	6.0	0.3	0.5–8.0	[46]
GOD/polyurethane/GCE	0.6	1.3	0.1	0.1–60	[47]
GOD/Pt–C[e]/Nafion/GCE	0.8	125	0.3	0–40	[48]

[a] Mesocellular silica–carbon nanocompositefoam.
[b] Nitrogen-doped carbon nanotubes.
[c] Polydopamine.
[d] Flower-like carbon nanosheet aggregation.
[e] Carbon vulcan.

3.5. Reproducibility and stability of the GOD–MSN/Nafion/GCE

The reproducibility of the GOD–MSN/Nafion/GCE was investigated by successive detection of 0.1 mM glucose for eight times. The relative standard deviation (*RSD*) was 2.9%. The fabrication reproducibility of the proposed enzyme electrode was also assessed by measuring 0.1 mM glucose at eight different modified electrodes, and the obtained *RSD* was 4.2%. After 30 successive detections the response was still retained 97% value of the initial response, suggesting the acceptable operational stability of the GOD–MSN/Nafion/GCE. After a storage period of 20 days in 0.1 M pH 7.0 PBS at 4 °C, the fabricated enzyme electrode showed a 6.5% loss of bioactivity. These results indicate that the immobilized GOD retains its high enzymatic activity, which was very important for the development of the proposed enzyme electrode in low-cost application.

3.6. Interference study and detection of glucose in practical serum sample

The interferences in glucose detection were evaluated using 0.2 mM ascorbic acid (AA), 0.2 mM uric acid (UA) and 0.2 mM acetaminophen (AP) at the applied potential of −0.45 V (Fig. 8). Upon addition of 0.2 mM glucose in pH 6.5 air-saturated PBS, an obvious current response was observed. After successively injecting the AA, UA and AP into the electrolyte solution, no obvious change of the current response was observed. The presence of Nafion in the matrix can prevent both enzyme leakage and diffusion of the interferences, leading to an improved selectivity [48]. When adding 0.2 mM glucose in PBS again, the current value was close to that detected in absence of the interferents. These results demonstrates that the proposed GOD–MSN/Nafion/GCE has high selectivity for glucose in the presence of those endogenously coexisted electroactive substances.

To assess the practical application of the GOD–MSN/Nafion/GCE, the detection of glucose in nine serum samples was carried out using the proposed method as well as the reference method. The serum samples were received from a local hospital without any sample pretreatment except a dilution step. The reference glucose levels were determined by local hospital using an Automatic Biochemical Analyzer (7170 A, Hitachi). When the level of glucose in serum sample is over linear range, serum sample are diluted appropriately with 0.01 M pH 7.4 PBS prior to detection. The relative errors between the two methods were all less than 4.6% (Table 2), indicating the good accuracy for detection of glucose in real samples.

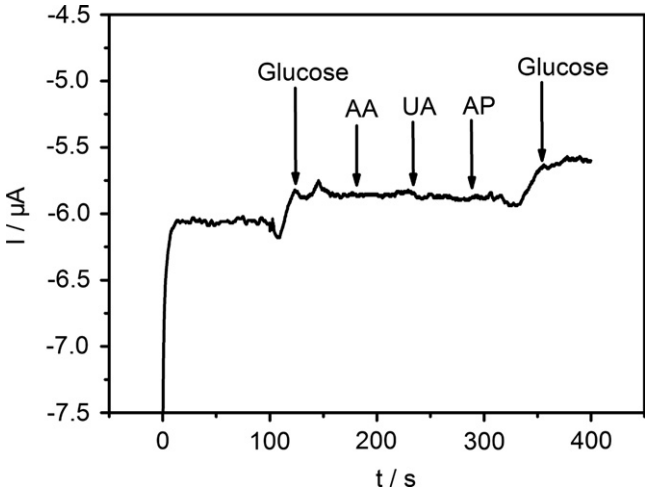

Fig. 8. Amperometric response of the GOD–MSN/Nafion/GCE to 0.2 mM glucose, 0.2 mM AA, 0.2 mM UA and 0.2 mM AP in pH 6.5 PBS at −0.45 applied potential.

Table 2
Detection results of glucose concentrations in clinical serum samples.

Samples	Proposed method (mM)	Reference method (mM)	Relative errors (%)
1	4.24	4.40	3.6
2	4.70	4.80	2.1
3	4.96	5.20	4.6
4	5.69	5.90	3.6
5	6.74	6.90	2.3
6	6.93	7.10	2.4
7	8.00	8.20	2.5
8	10.9	11.0	0.9
9	12.8	13.0	1.5

4. Conclusions

A novel glucose biosensor was proposed based on immobilizing GOD at mesoporous silica nanosphere modified electrode. The mesoporous silica nanosphere matrix has large specific surface area and uniform mesoporous structure, which are advantageous to obtain a high enzyme loading. Moreover, the mesoporous silica materials provide a favorable microenvironment for facilitating the direct electron transfer between the enzyme and the electrode surface. The immobilized enzyme on mesoporous silica nanosphere exhibits fast electrochemical response to glucose. The

fabricated enzyme biosensor has wide linear range, low detection limit, excellent selectivity and good reproducibility and stability. The mesoporous silica nanosphere matrix opens a new avenue for immobilizing proteins and fabrication of excellent electrochemical biosensors.

Acknowledgments

This work was financially supported by National Natural Science Foundation of China (Nos. 20973151, 21273195, 21103148 and 21005070), The Priority Academic Program Development of Jiangsu Higher Education Institution, Postdoctoral Science Foundation of China (Nos. 20110491462, 2012T50519), Postdoctoral Science Foundation of Jiangsu Province (Nos. 1101020B, 1102142C) and the Open Research Fund of State Key Laboratory of Bioelectronics of Southeast University (No. 2011E13).

Appendix A. Supporting information

Supplementary data associated with this article can be found in the online version at http://dx.doi.org/10.1016/j.talanta.2012.11.038.

References

[1] C.T. Kresge, M.E. Leonowicz, W.J. Roth, J.C. Vartuli, J.S. Beck, Nature 359 (1992) 710.
[2] J.E. Lee, D.J. Lee, N. Lee, B.H. Kim, S.H. Choi, T. Hyeon, J. Mater. Chem. 21 (2011) 16869.
[3] J.X. Li, Z.Y. Xiong, L.H. Zhou, X. Han, H.L. Liu, Micropor. Mesopor. Mater. 130 (2010) 333.
[4] C.Y. Lai, B.G. Trewyn, D.M. Jeftinija, K. Jeftinija, S. Xu, S. Jeftinija, V.S.Y. Lin, J. Am. Chem. Soc. 125 (2003) 4451.
[5] Q.J. He, J.L. Shi, J. Mater. Chem. 21 (2011) 5845.
[6] M. Vallet-Regi, A. Ramila, R.P. del Real, J. Perez-Pariente, Chem. Mater. 13 (2001) 308.
[7] M. Vallet-Regi, F. Balas, D. Arcos, Angew. Chem. Int. Ed. 46 (2007) 7548.
[8] I.I. Slowing, J.L. Vivero-Escoto, C.W. Wu, V.S.Y. Lin, Adv. Drug Deliv. Rev. 60 (2008) 1278.
[9] M. Manzano, M. Vallet-Regi, J. Mater. Chem. 20 (2010) 5593.
[10] Q.J. He, J.L. Shi, F. Chen, M. Zhu, L.X. Zhang, Biomaterials 31 (2010) 3335.
[11] M. Liong, J. Lu, M. Kovochich, T. Xia, S.G. Ruehm, A.E. Nel, F. Tamanoi, J.I. Zink, ACS Nano 2 (2008) 889.
[12] I.I. Slowing, B.G. Trewyn, S. Giri, V.S.Y. Lin, Adv. Funct. Mater. 17 (2007) 1225.
[13] B.G. Trewyn, S. Giri, I.I. Slowing, V.S.Y. Lin, Chem. Commun. 31 (2007) 3236.
[14] Y.S. Lin, C.P. Tsai, H.Y. Huang, C.T. Kuo, Y. Hung, D.M. Huang, Y.C. Chen, C.Y. Mou, Chem. Mater. 17 (2005) 4570.
[15] C.P. Tsai, Y. Hung, Y.H. Chou, D.M. Huang, J.K. Hsiao, C. Chang, Y.C. Chen, C.Y. Mou, Small 4 (2008) 186.
[16] Z.H. Dai, J. Ni, X.H. Huang, G.F. Lu, J.C. Bao, Bioelectrochemistry 70 (2007) 250.
[17] K.C. Kao, C.H. Lee, T.S. Lin, C.Y. Mou, J. Mater. Chem. 20 (2010) 4653.
[18] Y. Xiao, F. Patolsky, E. Katz, J.F. Hainfeld, I. Willner, Science 299 (2003) 1877.
[19] S. Wu, H.X. Ju, Y. Liu, Adv. Funct. Mater. 17 (2007) 585.
[20] V. Vamvakai, K. Tsagaraki, N. Chaniotakis, Anal. Chem. 78 (2006) 5538.
[21] X.C. Chu, B.H. Wu, C.H. Xiao, X.H. Zhang, J.H. Chen, Electrochim. Acta 55 (2010) 2848.
[22] X.A. Xu, S.J. Jiang, Z. Hu, S.Q. Liu, ACS Nano 4 (2010) 4292.
[23] J. Wang, Chem. Rev. 108 (2008) 814.
[24] L. Meng, J. Jin, G.X. Yang, T.H. Lu, H. Zhang, C.X. Cai, Anal. Chem. 81 (2009) 7271.
[25] F. Jia, C.S. Shan, F.H. Li, L. Niu, Biosens. Bioelectron. 24 (2008) 945.
[26] J.M. Pingarron, P. Yanez-Sedeno, A. Gonzalez-Cortes, Electrochim. Acta 53 (2008) 5848.
[27] B.R. Azamian, J.J. Davis, K.S. Coleman, C.B. Bagshaw, M.L.H. Green, J. Am. Chem. Soc. 124 (2002) 12664.
[28] D. Wen, Y. Liu, G.C. Yang, S.J. Dong, Electrochim. Acta 52 (2007) 5312.
[29] J. Wang, M. Miasma, Anal. Chem. 75 (2003) 2075.
[30] M. Ammam, J. Fransaer, Biotechnol. Bioeng. 109 (2012) 1601.
[31] C.S. Shan, H.F. Yang, D.X. Han, Q. Zhang, A. Ivaska, L. Niu, Biosens. Bioelectron. 25 (2010) 1070.
[32] X.H. Kang, J. Wang, H. Wu, I.A. Aksay, J. Liu, Y.H. Lin, Biosens. Bioelectron. 25 (2009) 901.
[33] S.J. Bao, C. Li, J.F. Zang, X.Q. Cui, Y. Qiao, J. Guo, Adv. Funct. Mater. 18 (2008) 591.
[34] Z.J. Yang, Y.Y. Ren, Y.C. Zhang, J. Li, H.B. Li, X.C. Huang, X.Y. Hu, Q. Xu, Biosens. Bioelectron. 26 (2011) 4337.
[35] H.Y. Liu, N.F. Hu, Electroanalysis 19 (2007) 884.
[36] S.Q. Liu, H.X. Ju, Biosens. Bioelectron. 19 (2003) 177.
[37] J. Bard, L.R. Faulkner, Electrochemistry Methods, 2nd ed., Wiley, New York, 2001.
[38] Y.H. Wu, S.S. Hu, Bioelectrochemistry 70 (2007) 335.
[39] J.Z. Xu, J.J. Zhu, Q. Wu, Z. Hu, H.Y. Chen, Chin. J. Chem. 21 (2003) 1088.
[40] Z.J. Yang, X.C. Huang, Y.C. Zhang, J. Li, Q. Xu, X.Y. Hu, Electrochim. Acta 70 (2012) 325.
[41] C.Y. Deng, J.H. Chen, X.L. Chen, C.H. Xiao, L.H. Nie, S.Z. Yao, Biosens. Bioelectron. 23 (2008) 1272.
[42] A. Guiseppi-Elie, C. Lei, R.H. Baughman, Nanotechnology 13 (2002) 559.
[43] S.Y. Deng, G.Q. Jian, J.P. Lei, Z. Hu, H.X. Ju, Biosens. Bioelectron. 25 (2009) 373.
[44] X.L. Ren, D. Chen, X.W. Meng, F.Q. Tang, A.M. Du, L. Zhang, Colloids Surf. B 72 (2009) 188.
[45] C.H. Xiao, X.C. Chu, B.H. Wu, H.L. Pang, X.H. Zhang, J.H. Chen, Talanta 80 (2010) 1719.
[46] S. Tang, X.Z. Wang, J.P. Lei, Z. Hu, S.Y. Deng, H.X. Ju, Biosens. Bioelectron. 26 (2010) 432.
[47] M. Amman, J. Fransaer, Sens. Actuators B 145 (2010) 46.
[48] M. Ammam, E.B. Easton, Sens. Actuators B 155 (2011) 340.
[49] C.H. Xiao, X.C. Chu, B.H. Wu, H.L. Pang, X.H. Zhang, J.H. Chen, Talanta 80 (2010) 1719.
[50] H. Zheng, H. Xue, Y. Zhang, Z. Shen, Biosens. Bioelectron. 17 (2002) 541.
[51] Y. Uang, T.C. Chou, Biosens. Bioelectron. 20 (2003) 2435.